

# Exploring the Potential of High Entropy Alloys: A Comprehensive Review on Microstructure, Properties and Applications: Part II

**Properties, applications, remaining challenges and future directions**

## S. Arun

Department of Mechanical Engineering, Amrita School of Engineering, Coimbatore, Amrita Vishwa Vidyapeetham, India; Department of Mechanical Engineering, MES College of Engineering, Kuttippuram, Kerala, India

## N. Radhika\*

Department of Mechanical Engineering, Amrita School of Engineering, Coimbatore, Amrita Vishwa Vidyapeetham, India

## Bassiouny Saleh

College of Energy and Power Engineering, Nanjing University of Aeronautics and Astronautics, Nanjing 210016, China; Production Engineering Department, Alexandria University, Alexandria 21544, Egypt

\*Email: [n\\_radhika1@cb.amrita.edu](mailto:n_radhika1@cb.amrita.edu)

## PEER REVIEWED

Received 30th November 2024; Revised 31st January 2024; Accepted 7th February 2024; Online 7th February 2024

This is Part II of a comprehensive review analysing recent studies on various high entropy alloys (HEAs). Here, we present their magnetic and electrical properties, corrosion resistance, wear behaviour and different applications. Remaining challenges and perspectives are summarised. The anticipated findings of this two-part review are a milestone for future investigations on the

production and analysis of HEAs. The discoveries hold great value for researchers, designers and manufacturers working in this field, as they offer valuable knowledge regarding the characteristics and possible uses of HEAs. Consequently, these findings lay the groundwork for further exploration in this promising field of materials science.

## Keywords

high entropy alloys, microstructure, properties, applications, future directions

## 1. Evaluation of High Entropy Alloys

Part I (1) began the discussion of HEAs properties. Here, we continue their evaluation.

### 1.1 Magnetic Properties Evaluation

Magnets play a crucial role in the functionality of many everyday instruments and devices (2–5). Even a slight alteration in their magnetic properties can have a substantial impact on their performance, resulting in increased energy efficiency and cost effectiveness. To improve the quality of the soft magnetic material (core material), it is essential to ensure that it has high saturation magnetisation ( $M_s$ ), low coercivity ( $H_c$ ), high electrical resistivity (to minimise eddy current loss) and an optimal balance of magnetic and mechanical properties. With the inclusion of multiple principal elements, magnetic HEAs have significant potential for property tuning. The magnetic properties of HEAs which have recently reported, are extremely good (6, 7).

For functional applications, materials with very good magnetic properties are desirable. The most important constituent elements found in alloys while they are investigated for their magnetic properties are iron, cobalt and nickel (8). Investigating magnetic properties of aluminium and silicon addition on equal atomic CoFeNi alloys reveals a ferromagnetic behaviour. In these alloys, saturation magnetisation ( $M_s$ ) values demonstrated an increase with higher aluminium or silicon content, as seen in **Figure 1(a)** (9). In the case of  $\text{Co}_x\text{CrCuFeMnNi}$  HEA powders prepared using mechanical alloying,  $M_s$  values increased from  $21 \text{ emu g}^{-1}$  to  $52 \text{ emu g}^{-1}$  when copper content was increased from 0.5 to 2.0 while coercivity force ( $H_c$ ) decreased from 63 Oe to 14 Oe and remanence ratio ( $M_r:M_s$ ) decreased from 16% to 3% with an increase in copper content. Soft magnetic properties of  $\text{Co}_2\text{CrCuFeMnNi}$  were superior among the four HEA powders investigated (11).

Upon investigating  $\text{CoFeMnNiX}$  magnetic alloys prepared using an arc melting process, it was discovered that the introduction of elements such as aluminium, chromium, gallium or tin into the alloy system caused a transition in the phase structure from fcc to ordered bcc. This change resulted in an improvement in the saturated magnetisation of the alloy system. The behaviour exhibited by the alloy system was found to be ferromagnetic when

aluminium, gallium, or tin was added, while the  $\text{CoFeMnNiCr}$  alloy system exhibited paramagnetic-like behaviour (12). Studies carried out on magnetic properties of  $\text{FeCoNi(AlMn)}_x$  alloys prepared using arc melting process show that when AlMn content is increased, the phase exhibited was as that of bcc, which resulted in very good magnetic properties (13).  $\text{TiFeNiCr}$ ,  $\text{TiFeNiCrMn}$  and  $\text{TiFeNiCrCo}$  HEAs prepared using mechanical alloying exhibited soft magnetic characteristics. Saturation magnetisation of these alloys increased with an increase in ferromagnetic element content in the alloy system (14). Magnetic behaviour investigation soft magnetic behaviour was observed in  $\text{AlCoCrCuFeNi}$  HEAs. While  $M_s$ ,  $H_c$  and remanence ratio are higher for aged alloy. This was due to the fact that the degree of decomposition was much greater in Cr-Fe-Co-rich regions (15).

**Figures 1(b)** and **1(c)** show the room temperature magnetic hysteresis loop of  $\text{FeCoNiMnV}$  HEA milled at different milling times. By taking into account that the  $\text{FeCoNiMnV}$  alloys produced with varying milling times magnetise up to a saturation state of  $100 \text{ emu g}^{-1}$  with a coercivity below 150 Oe, one can observe their semi-hard magnetic properties. For the samples milled for up to 48 h, the saturation magnetisation values increase to a value of  $100 \text{ emu g}^{-1}$ . Further increase in milling time decreases the saturation magnetisation values (10).

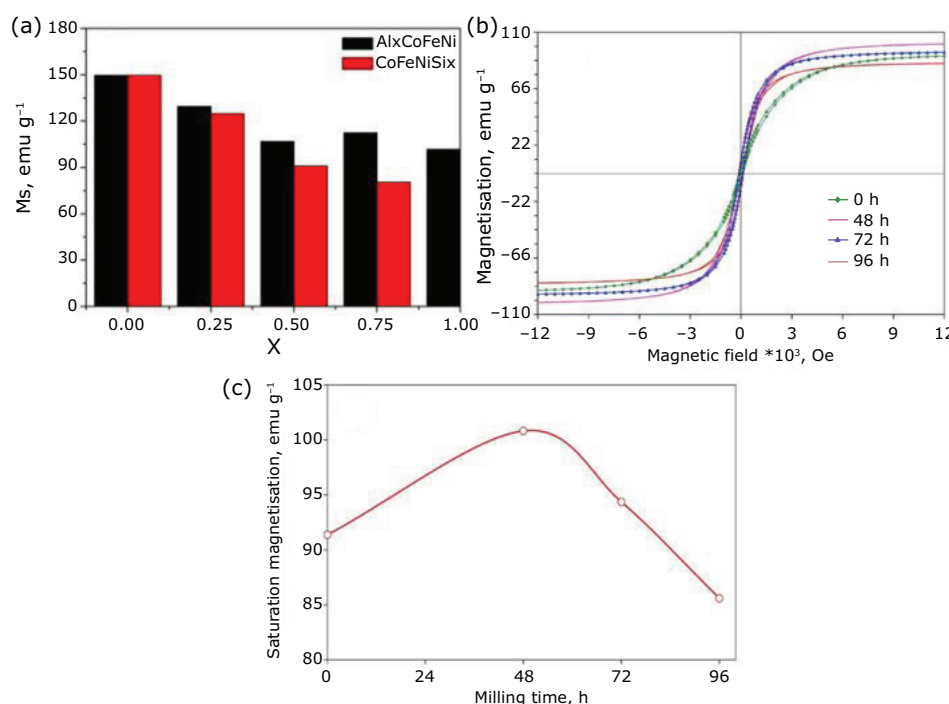


Fig. 1. (a) Variation of saturated magnetisation ( $M_s$ ) with change in aluminium in  $\text{Al}_x\text{CoFeNi}$  and Si in  $\text{CoFeNiSi}_x$  alloys; (b) magnetic hysteresis loop; (c) variation of  $M_s$  with milling time of  $\text{FeCoNiMnV}$  HEA. Reprinted from (9, 10) with permission from Elsevier

## 1.2 Electrical and Thermal Properties Evaluation

Studies carried out on  $\text{AlCu}_x\text{NiTiZr}_{0.75}$  HEA films for their electrical resistivity reveal that the highest resistivity for  $\text{AlCuNiTiZr}_{0.75}$  and the value is around  $363 \mu\Omega \text{ cm}$  as seen in **Figure 2(a)**. As the copper content increased, the resistance of the HEA films exhibited a significant decrease. Hence, this alloy can be considered a good alternative for applications related to electrical conductivity (16).  $\text{TiZrHfNb}$  HEA prepared using an arc melting process, when investigated for its electrical resistance behaviour in a pressure range of 0 GPa to 5.41 GPa, reveals that it is heavily influenced by pressure, but the temperature does not have an influence on its resistance (21). With the increase in initial current density, on a rapidly quenched  $\text{CrMnFeCoNi}$  HEA, that resistivity decreased slightly initially and then increased with repeated electroplating (22). When the AlN mass fraction is increased in AlN-CoCrFeMnNi cermets, electrical resistivity shows an increasing trend, as seen in **Figure 2(b)** and **2(c)**. A similar trend can be observed when the temperature is increased (17).

The electrical resistivity of NbMoTaW RHEA thin film was observed to be  $168 \mu\Omega \text{ cm}$ . The reason for the high value of resistivity is due to the nanoscale microstructure and the high degree of lattice distortion (23). **Figure 2(d)** reveals the electrical resistivity plots of VNbMoTaW HEA films on sapphire and 304 stainless steel substrates. Even when exposed to a temperature of  $800^\circ\text{C}$ , VNbMoTaW HEA thin films can help keep the apparent resistivity of a 304 stainless steel substrate low. The corresponding total apparent resistivity values are  $5.80 \Omega \text{ cm}$ ,  $6.91 \Omega \text{ cm}$  and  $7.71 \Omega \text{ cm}$  at  $600^\circ\text{C}$ ,  $700^\circ\text{C}$  and  $800^\circ\text{C}$ , respectively (18). The conductivity of electricity in materials is typically linked to imperfections in their microstructure and distortions in their lattice structure, which results in the scattering of electrons (24). Additionally, the degree of distortion in the lattice can cause the electrical resistivity of alloys to vary (25). Thermal stability carried on bcc MoNbTaVW HEA thin films prepared using a cathodic arc deposition method reveals that up to a temperature of  $1500^\circ\text{C}$  solid solution phase is stable. As seen in **Figure 2(e)**, for as-deposited alloys, elastic modulus values are independent of annealing temperature in a vacuum, but hardness values decreased with increasing the annealing temperature (19). As seen in **Figure 2(f)** there is a linear increase in the dilatometry coefficient of thermal expansion

up to  $800^\circ\text{C}$  for  $\text{FeCoCrNi}_2\text{Al}$  HEA. The  $\text{FeCoCrNi}_2\text{Al}$  HEA displayed a linear relationship between temperature and thermal expansion behaviour up to  $800^\circ\text{C}$ . However, beyond this temperature, there was a deviation from linearity in the thermal expansion response. The observed deviation from linearity in the thermal expansion behaviour of the  $\text{FeCoCrNi}_2\text{Al}$  HEA at temperatures above  $800^\circ\text{C}$  can be attributed to the increased presence of a BCC face with a higher concentration of nickel and aluminium. Despite this deviation, the material exhibits a steady and linear thermal expansion behaviour, making it suitable for high-temperature applications (20).

## 1.3 Corrosion Resistance Evaluation

Corrosion is a progressive phenomenon wherein metals undergo degradation due to chemical or electrochemical reactions, such as exposure to air or water. This leads to the formation of more stable compounds like hydroxides, sulfides or oxides, which can result in a loss of strength and affect the appearance and functionality of the metal. To avoid safety hazards in equipment and structures, it is crucial to prevent and control corrosion in many industries. In highly corrosive solutions with high sulfuric acid concentration, hydrochloric acid concentration and other harsh conditions, HEAs have demonstrated excellent corrosion resistance. **Table I** illustrates that HEA coatings can significantly enhance the corrosion resistance of copper substrates.

Various parameters of HEAs in sodium chloride solution obtained from the potentiodynamic polarisation tests are summarised in **Table II**. It reveals that corrosion current density increases as aluminium content is increased in  $\text{Al}_x\text{CoCrFeNi}$  alloy, while pitting potential decreases, indicating degradation of corrosion resistance of the alloy. The corrosion resistance of alloys differed greatly depending on the amount of silicon content. Out of various silicon-doped alloys, one which has better corrosion resistance is  $\text{Co}_{0.2}\text{CrAlSi}_{0.1}\text{Ni}$  alloy. Since the reduction in the  $\text{Cr}^{3+}$  on the surface of the alloys, the formation of passivation films is obstructed by the excessive addition of silicon into the alloy. During alloy polarisation, preferential corrosion of the B2 phase occurs. The incorporation of a small amount of silicon ( $x = 0.1$ ) into HEAs was found to have a minimal negative impact on their corrosion resistance. The corrosion resistance of  $\text{AlCu}_x\text{NiTiZr}_{0.75}$  HEA films decreases as the copper content increases. This reduction in corrosion resistance can be attributed to

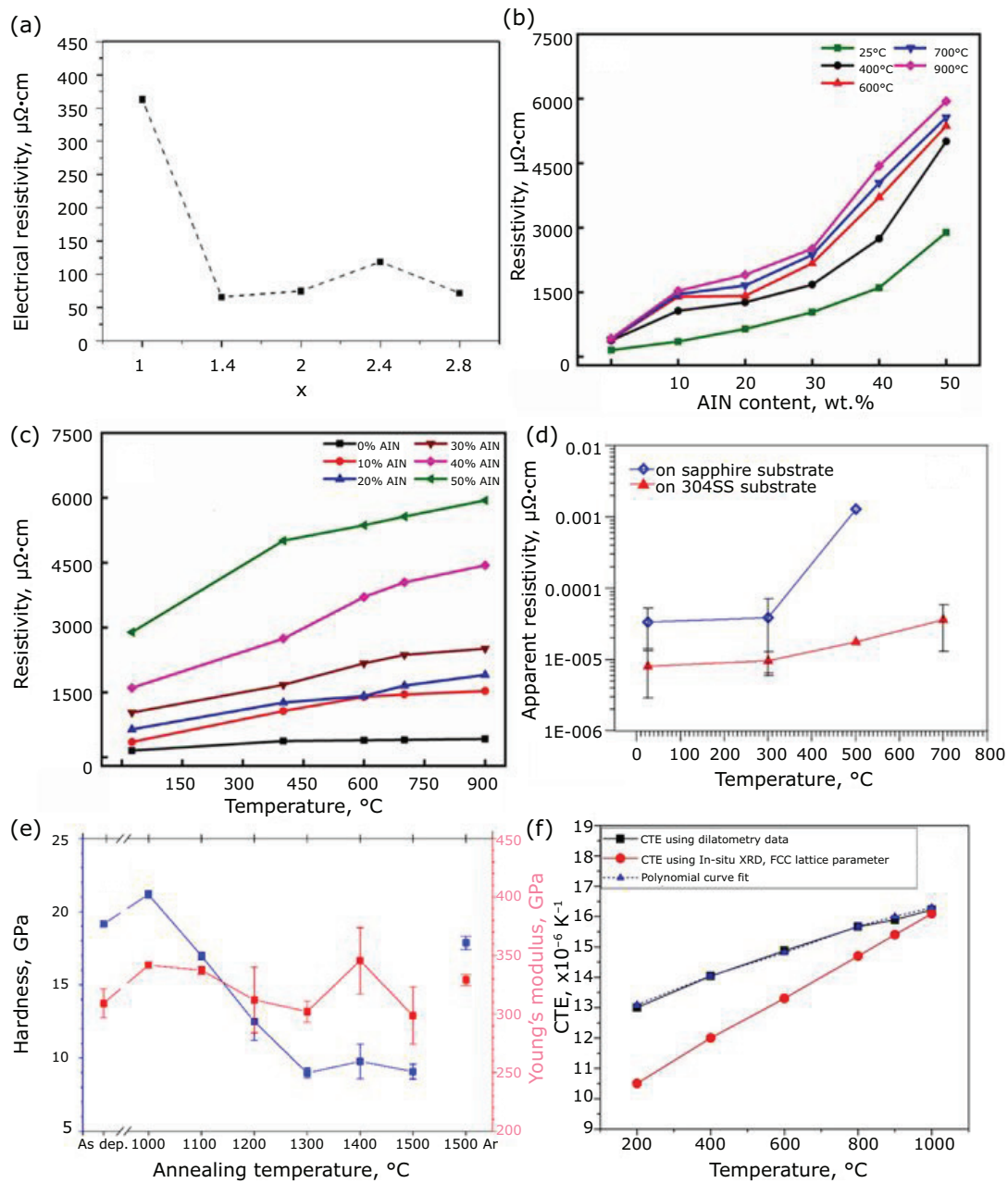


Fig. 2. (a) Variation of electrical resistivity of  $\text{AlCu}_x\text{NiTiZr}_{0.75}$  HEA films with variation in copper content; (b) variation of electrical resistivity in  $\text{AlN-CoCrFeMnNi}$  Cermets with change in AlN content; (c) variation of electrical resistivity in  $\text{AlN-CoCrFeMnNi}$  Cermets with change in temperature; (d) electrical resistivity versus oxidation temperature of  $\text{VNbMoTaW}$  HEA films; (e) hardness and Youngs modulus of  $\text{MoNbTaVW}$  thin films on  $\text{Al}_2\text{O}_3$  substrates with varying annealing temperature; (f) coefficient of thermal expansion calculated using various methods for  $\text{FeCoCrNi}_2\text{Al}$  HEA (16–20)

**Table I Electrochemical Parameters in 3.5 wt% Sodium Chloride Solution of Copper Substrate, FeCoNiCr, FeCoNiCrMn and FeCoNiCrAl HEA Coatings (26)**

| Material                               | Copper substrate                | FeCoNiCr HEA coatings           | FeCoNiCrMn HEA coatings         | FeCoNiCrAl HEA coatings         |
|--|---------------------------------|---------------------------------|---------------------------------|---------------------------------|
| $E_{\text{corr}}$ , V                  | $-0.831 \pm 0.001$              | $-0.508 \pm 0.001$              | $-0.402 \pm 0.002$              | $-0.392 \pm 0.001$              |
| $I_{\text{corr}}$ , $\text{A cm}^{-2}$ | $6.252 \times 10^{-5} \pm 0.16$ | $3.327 \times 10^{-5} \pm 0.21$ | $5.794 \times 10^{-5} \pm 0.11$ | $1.772 \times 10^{-5} \pm 0.16$ |

**Table II Electrochemical Parameters of High-Entropy Alloys in 3.5 wt% Sodium Chloride Solution**

| Alloy  | $E_{corr}$ V          | $I_{corr}$ $\mu\text{A cm}^{-2}$ | $E_{pitr}$ V         | Ref. |
|--|-----------------------|----------------------------------|----------------------|------|
| $\text{Al}_{0.3}\text{CoCrFeNi}$                   | -195 ( $\pm 8$ )      | 0.0835 ( $\pm 0.027$ )           | 460 ( $\pm 18$ )     | (30) |
| $\text{Al}_{0.5}\text{CoCrFeNi}$                   | -225 ( $\pm 14$ )     | 0.252 ( $\pm 0.046$ )            | 385 ( $\pm 36$ )     |      |
| $\text{Al}_{0.7}\text{CoCrFeNi}$                   | -275 ( $\pm 9$ )      | 0.429 ( $\pm 0.054$ )            | 52 ( $\pm 12$ )      |      |
| $\text{Co}_{0.2}\text{CrAlNi}$                     | -0.38                 | 0.526                            | -                    | (28) |
| $\text{Co}_{0.2}\text{CrAlSi}_{0.1}\text{Ni}$      | -0.37                 | 1.15                             | -                    |      |
| $\text{Co}_{0.2}\text{CrAlSi}_{0.3}\text{Ni}$      | -0.39                 | 0.117                            | -                    |      |
| $\text{Co}_{0.2}\text{CrAlSi}_{0.5}\text{Ni}$      | -0.46                 | 0.390                            | -                    |      |
| $\text{Co}_{0.2}\text{CrAlSi}_{0.7}\text{Ni}$      | -0.37                 | 0.25                             | -                    |      |
| $\text{FeCoNiCr}$                                  | -0.46                 | 0.035                            | 0.31                 | (27) |
| $\text{FeCoNiCrCu}_{0.5}$                          | -0.49                 | 0.72                             | 0.09                 |      |
| $\text{FeCoNiCrCu}$                                | -0.53                 | 1.23                             | 0.08                 |      |
| $(\text{CoCrFeNi})_{95}\text{Nb}_5$                | -0.37                 | 7.23                             | 0.26                 | (29) |
| $\text{AlCuNiTrZr}_{0.75}$                         | -0.31                 | 0.0769                           | -                    | (16) |
| $\text{AlCu}_2\text{NiTrZr}_{0.75}$                | -0.36                 | 0.363                            | -                    |      |
| $\text{AlCu}_{2.8}\text{NiTrZr}_{0.75}$            | -0.37                 | 1.10                             | -                    |      |
| $\text{FeCoNiCrMn}$                                | -0.30( $\pm 0.003$ )  | 0.476( $\pm 0.07$ )              | 0.130( $\pm 0.003$ ) | (31) |
| $\text{FeCoNiCrMnW}_{0.2}$                         | -0.292( $\pm 0.002$ ) | 0.181( $\pm 0.03$ )              | 0.046( $\pm 0.003$ ) |      |
| $\text{FeCoNiCrMnW}_{0.4}$                         | -0.274( $\pm 0.002$ ) | 0.190( $\pm 0.04$ )              | 0.159( $\pm 0.003$ ) |      |
| $\text{FeCoNiCrMnW}_{0.6}$                         | -0.271( $\pm 0.002$ ) | 0.211( $\pm 0.04$ )              | 0.168( $\pm 0.002$ ) |      |
| $\text{FeCoNiCrMnW}_{0.8}$                         | -0.264( $\pm 0.003$ ) | 0.168( $\pm 0.02$ )              | 0.199( $\pm 0.001$ ) |      |
| $\text{FeCoNiCrMnW}_1$                             | -0.282( $\pm 0.002$ ) | 0.274( $\pm 0.02$ )              | 0.162( $\pm 0.003$ ) |      |
| $\text{Al}_0\text{CrFeVMo}$                        | -0.397                | 0.117                            | 0.992                | (32) |
| $\text{Al}_{0.2}\text{CrFeVMo}$                    | -0.410                | 0.077                            | 1.025                |      |
| $\text{Al}_{0.6}\text{CrFeVMo}$                    | -0.460                | 0.320                            | 1.004                |      |
| $\text{Al}_1\text{CrFeVMo}$                        | -0.307                | 0.082                            | 0.993                |      |
| $\text{Al}_{0.3}\text{CoCrFeNi (As forged)}$       | -0.189( $\pm 0.01$ )  | 0.0632( $\pm 0.0275$ )           | 0.052( $\pm 0.018$ ) | (33) |
| $\text{Al}_{0.5}\text{CoCrFeNi (As forged)}$       | -0.261( $\pm 0.008$ ) | 0.187( $\pm 0.046$ )             | 0.316( $\pm 0.032$ ) |      |
| $\text{Al}_{0.7}\text{CoCrFeNi (As forged)}$       | -0.292( $\pm 0.008$ ) | 0.392( $\pm 0.054$ )             | 0.118( $\pm 0.012$ ) |      |
| $\text{Al}_{0.3}\text{CoCrFeNi (As-equilibrated)}$ | -0.180( $\pm 0.012$ ) | 0.0289( $\pm 0.0066$ )           | 0.808( $\pm 0.016$ ) |      |
| $\text{Al}_{0.5}\text{CoCrFeNi (As-equilibrated)}$ | -0.228( $\pm 0.011$ ) | 0.0714( $\pm 0.0286$ )           | 0.496( $\pm 0.038$ ) |      |
| $\text{Al}_{0.7}\text{CoCrFeNi (As-equilibrated)}$ | -0.258( $\pm 0.008$ ) | 0.267( $\pm 0.052$ )             | 0.256( $\pm 0.010$ ) |      |
| $\text{FeCoCrAlNi}$                                | -0.167                | 0.073                            | 0.257                | (34) |

a decrease in the films' ability to withstand corrosion. Compared with the FeCoNiCrMn base, HEA corrosion resistance behaviour is improved with the addition of tungsten into the alloy.  $E_{corr}$  values of  $\text{Al}_x\text{CrFeVMo}$  HEAs decreased when aluminium content was increased from 0 to 0.6. However, aluminium content is 1,  $E_{corr}$  values of HEA are highest. This is due to the variation of bcc2 volume fraction in the matrix and its composition. There is a decrease in  $E_{corr}$  (corrosion potential) of  $\text{Al}_x\text{CoCrFeNi}$  HEAs with the increase in aluminium content in the alloy while its  $I_{corr}$  (corrosion current density) values increase. These trends indicate the weakening of corrosion resistance in a solution.

As seen in **Figure 3**, the FeCoCrAlNi HEA coating exhibits a noticeable enhancement in corrosion resistance when immersed in a 3.5% sodium chloride solution compared to the substrate material. The improved ability of the coating to resist corrosion may be explained by the presence of cobalt, chromium and nickel, which combine to create a protective layer. The FeCoCrAlNi HEA coating exhibits a cavitation erosion resistance ( $R_e$ ) approximately 7.6 times higher than that of 304 stainless steel. This improved resistance is likely due to the coating's optimal balance between hardness and toughness, which enables it to withstand intense cavitation pulses and results in

higher resistance to cavitation erosion (34). Initially, the corrosion resistance of the  $Al_xCrFeCoNiCu$  HEA coating in a 3.5% sodium chloride solution improved as the aluminium content increased, but then it declined. The optimum corrosion resistance was achieved with the  $Al_{0.8}$  coating. The corrosion mechanism involved severe pitting corrosion and intergranular corrosion (35).

As a result of the highest pitting potential value of  $1.099 \pm 0.014 V_{Ag/AgCl}$  for  $CoCrFeNiSn$  alloy when compared with  $CoCrFeNiCu$  ( $-0.069 \pm 0.009 V_{Ag/AgCl}$ ) and  $CoCrFeNiAl$  ( $0.297 \pm 0.040 V_{Ag/AgCl}$ ) alloys. At room temperature,  $CoCrFeNiSn$  alloy has better corrosion resistance in 0.6 M sodium chloride solution (36). The corrosion characteristics analysis revealed that the  $FeCrSiNb$  HEA thin film

displayed superior corrosion resistance compared to 304 stainless steel. This was evident from its higher corrosion potential observed in various corrosive environments such as sodium chloride, sulfuric acid and crude oil (37). **Table III** summarises the corrosion behaviour of various HEAs in 0.5 M sulfuric acid solution. It is seen that with the addition of molybdenum, corrosion current density tends to increase. When the zirconium content is increased in  $AlCoCrFeNiZr_x$  alloys, the corrosion resistance first increases and then shows a decreasing trend. In 0.1 M sulfuric acid solution, the non-equiatomic  $Fe_{40}Ni_{20}Co_{20}Cr_{20}$  HEA exhibits higher electrochemical corrosion resistance compared to 316L stainless steel (41). The corrosion current densities of  $AlCoCuFeNi$  and aluminium  $CoCuFeNiCr$  HEAs have lower values when compared with  $AlCoCuFeNiTi$  and  $AlCoCuFeNiCrTi$  HEAs. The corrosion resistance of  $FeNiCoCuAl$  HEAs decreased with the incorporation of titanium into the alloy system. Conversely, the inclusion of chromium improved the corrosion resistance of  $FeNiCoCuAl$  HEAs without titanium (38).

$E_b$ : potential difference between corrosion potential and breakdown potential.

As seen in **Table IV**, the corrosion resistance of  $Al_2CrFeNiCoCuTi_x$  HEA coatings demonstrates improvement as the titanium content within the alloy increases. Laser cladded  $Al_xFeCoNiCrTi$  coatings exhibit much higher corrosion resistance than 314L stainless steel. The immersion and potentiodynamic polarisation tests carried out in  $Cu_{40}Mn_{25}Al_{20}Fe_5Co_5Ni_5$  HEAs reveal that as the concentration of  $HNO_3$  is increased from 0.5% to 10%, the corrosion rate increases (44).

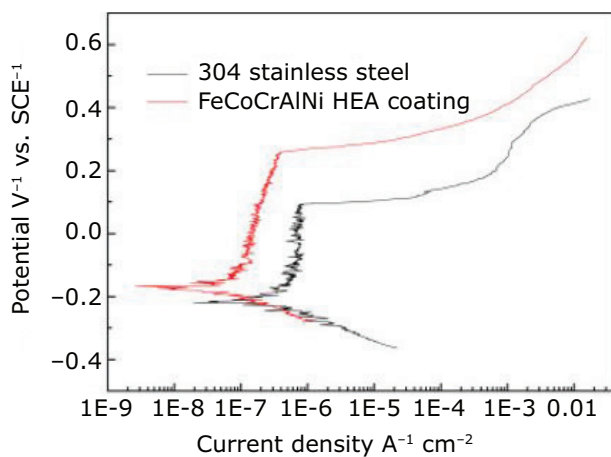


Fig. 3. The potentiodynamic polarisation curves for both 304 stainless steel and FeCoCrAlNi HEA coating measured in a solution containing 3.5% NaCl (34)

| Table III Electrochemical Parameters of HEAs in 0.5 M Sulfuric Acid Solution |                     |                           |                |      |  |  |
|--|---------------------|---------------------------|----------------|------|--|--|
| Alloy  | $E_{corr}/ V_{SHE}$ | $I_{corr}/ \mu A cm^{-2}$ | $E_b/ V_{SHE}$ | Ref. |  |  |
| $Co_{1.5}CrFeNi_{1.5}Ti_{0.5}$   | -0.092              | 30                        | 1.130          | (39) |  |  |
| $Co_{1.5}CrFeNi_{1.5}Ti_{0.5}Mo_{0.1}$                                       | -0.071              | 78                        | 1.112          |      |  |  |
| $Co_{1.5}CrFeNi_{1.5}Ti_{0.5}Mo_{0.5}$                                       | -0.064              | 72                        | 1.109          |      |  |  |
| $Co_{1.5}CrFeNi_{1.5}Ti_{0.5}Mo_{0.8}$                                       | -0.070              | 69                        | 1.109          |      |  |  |
| $AlCoCrFeNi$   | -0.491              | 230                       | -              | (40) |  |  |
| $AlCoCrFeNiZr_{0.1}$   | -0.510              | 102                       | -              |      |  |  |
| $AlCoCrFeNiZr_{0.3}$   | -0.525              | 406                       | -              |      |  |  |
| $AlCoCrFeNiZr_{0.5}$   | -0.489              | 136                       | -              |      |  |  |
| $AlCoCuFeNi$   | -0.058              | 7.93                      | -              | (38) |  |  |
| $AlCoCuFeNiCr$   | -0.075              | 5.09                      | -              |      |  |  |
| $AlCoCuFeNiTi$   | -0.253              | 44.76                     | -              |      |  |  |
| $AlCoCuFeNiCrTi$   | -0.256              | 39.59                     | -              |      |  |  |

The formation of passive films on alloy surfaces can provide protection against corrosion, but the presence of aluminium, copper or molybdenum can cause segregation and the formation of non-uniform passive films, leading to localised film breakdown. To improve corrosion resistance in saltwater environments, two strategies that can be employed are anodic treatment and the addition of molybdenum. HEAs subjected to high-temperature heat treatment can undergo a high-entropy effect that homogenises microstructures and compositions, eliminating elemental segregations and resulting in improved corrosion resistance. Certain high-entropy alloys display distinct corrosion behaviour when exposed to high-temperature and high-pressure water environments, suggesting their potential suitability for use in supercritical service conditions. HEA coatings fabricated using techniques such as laser cladding, electro-spark deposition and magnetron sputtering have showcased remarkable corrosion resistance. This can be attributed to the rapid cooling

process and the high-entropy effect associated with these coating methods. As a result, HEA coatings exhibit a more uniform microstructure and elemental distribution compared to bulk materials, contributing to their enhanced corrosion resistance properties.

### 1.4 Wear Resistance Evaluation

Wear is the process of continuous material removal from a surface due to mechanical action, shear force and friction that occur between adjacent surfaces. There are different forms of wear present in common use and it is a primary cause of failure for multiple components in numerous engineering applications. The distinctive compositions and diverse properties of HEA have caught the attention of numerous researchers, making it an appealing coating material for improving surface behaviour. The analysis of wear resistance can also involve examining the friction coefficient. **Table V** summarises the friction coefficient and wear rate

**Table IV Aqueous Environment Electrochemical Parameters of HEAs Coatings at Room Temperature**

| Alloy                                       | Solution                 | E <sub>corr</sub> | I <sub>corr</sub> A cm <sup>-2</sup> | Ref. |
|---|--------------------------|-------------------|--------------------------------------|------|
| Al <sub>2</sub> CrFeNiCoCu                  | 0.5 mol HNO <sub>3</sub> | -0.18             | 3.8×10 <sup>-2</sup>                 | (43) |
| Al <sub>2</sub> CrFeNiCoCuTi <sub>0.5</sub> | 0.5 mol HNO <sub>3</sub> | -0.30             | 2.2×10 <sup>-2</sup>                 |      |
| Al <sub>2</sub> CrFeNiCoCuTi <sub>1</sub>   | 0.5 mol HNO <sub>3</sub> | -0.33             | 7.3×10 <sup>-3</sup>                 |      |
| Al <sub>2</sub> CrFeNiCoCuTi <sub>1.5</sub> | 0.5 mol HNO <sub>3</sub> | -0.30             | 4.4×10 <sup>-3</sup>                 |      |
| Al <sub>2</sub> CrFeNiCoCuTi <sub>2</sub>   | 0.5 mol HNO <sub>3</sub> | -0.15             | 2.7×10 <sup>-3</sup>                 |      |
| AlFeCoNiCuCr                                | 0.05M HCl                | 0.55              | 2.92×10 <sup>-5</sup>                | (42) |
| Al <sub>1.3</sub> FeCoNiCuCr                | 0.05M HCl                | 0.58              | 4.79×10 <sup>-5</sup>                |      |
| Al <sub>1.5</sub> FeCoNiCuCr                | 0.05M HCl                | 0.92              | 3.14×10 <sup>-5</sup>                |      |
| Al <sub>1.8</sub> FeCoNiCuCr                | 0.05M HCl                | 0.673             | 0.76×10 <sup>-5</sup>                |      |
| Al <sub>2</sub> FeCoNiCuCr                  | 0.05M HCl                | 0.666             | 3.17×10 <sup>-5</sup>                |      |

**Table V Friction Coefficient and Wear Rate of Various HEAs**

| Alloy                                    | Friction coefficient | Wear rate × 10 <sup>-4</sup> , mm <sup>3</sup> Nm <sup>-1</sup> | Ref. |
|--|----------------------|---|------|
| As cast AlCoCrFeNi                       | 0.429                | 1.8   | (45) |
| Nitrided AlCoCrFeNi                      | 0.512                | 0.39  |      |
| As sprayed FeCoNiCrSiAl <sub>0.5</sub>   | 0.45                 | 0.55  | (46) |
| As sprayed FeCoNiCrSiAl                  | 0.45                 | 0.45  |      |
| As sprayed FeCoNiCrSiAl <sub>1.5</sub>   | 0.45                 | 0.3   |      |
| Heat treated FeCoNiCrSiAl <sub>0.5</sub> | 0.45                 | 0.016   |      |
| Heat treated FeCoNiCrSiAl                | 0.45                 | 0.067   |      |
| Heat treated FeCoNiCrSiAl <sub>1.5</sub> | 0.45                 | 0.081   | (47) |
| Al <sub>0.5</sub> CoCrFeNiSi             | 0.48                 | 0.0067  |      |
| Al <sub>1.0</sub> CoCrFeNiSi             | 0.39                 | 0.0058  |      |
| Al <sub>1.5</sub> CoCrFeNiSi             | 0.33                 | 0.0046  |      |
| Al <sub>2</sub> CoCrFeNiSi               | 0.24                 | 0.0032  |      |

of various reported HEAs. In comparison with as-cast AlCoCrFeNi HEAs, nitrided AlCoCrFeNi HEAs had a higher average friction coefficient. In the same conditions, the nitrided HEAs had a lower wear rate than the as-cast HEAs (45). As sprayed FeCoNiCrSiAl<sub>x</sub>, HEAs with a higher aluminium atom content are more resistant to wear. Heat-treated FeCoNiCrSiAl<sub>1.0</sub> HEA coatings exhibit higher wear resistance attributed to the formation of a bcc structure and the presence of the Cr<sub>3</sub>Ni<sub>5</sub>Si<sub>2</sub> phase (46). Al<sub>x</sub>CoCrFeNiSi HEA coatings are primarily subjected to abrasive wear and oxidative wear as the dominant wear mechanisms. However, the incorporation of aluminium into the HEA coatings contributes to improved wear resistance (47).

Compared to Q235 steel, as seen in **Figure 4(a)**, the relative wear resistance is much higher for Al<sub>2</sub>CrFeCoCuNiTi<sub>x</sub> HEA coatings. Wear resistance is highly influenced by both hardness and plasticity (43). The wear rate of the coated material decreases and the wear rate of the substrate increases as the frequency increases. This behaviour can be attributed to the presence of a hard silicide phase within a relatively ductile bcc matrix, which enhances the mechanical properties, particularly the hardness, of the coated material (49). The HEA coating on a titanium alloy substrate was composed of NiCrCoVTi<sub>0.5</sub>. The cladding process involved the use of a YLS-3000 laser to deposit the coating, followed by a re-melting step using two different laser power levels: 1 kW and 2 kW. This resulted in the formation of two distinct types of coatings on the substrate. The wear test was carried out at room temperature using a roller friction wear tester and the measurement of wear mass loss was performed. According to the results presented in **Figure 4(b)**, the wear test conducted on the cladded and reheated substrate revealed that among the various variables tested,

the as-remelted coating with a laser power of 1 kW exhibited the highest wear resistance. This coating experienced the lowest amount of mass loss compared to the other variables, indicating its superior performance in terms of wear resistance (48).

Erosion wear refers to the removal of material from a surface due to the repeated impact of small particles present in a moving fluid. This process is classified as an abrasive wear process. Extensive research on the erosion behaviour of high-entropy alloy coatings has been conducted, with a primary focus on two types of erosion: cavitation erosion and slurry erosion. For example, Ji *et al.* conducted an assessment of the slurry erosion characteristics of an AlCrFeCoNiCu HEA, which was produced using an arc melting process. The evaluation was performed using a jet erosion testing machine and the slurry flow utilised was composed of water and silica particles with a diameter range of 0.350–0.600 mm, with a concentration of 1% by weight. The mass loss and erosive wear resistance were observed to be 2.1 mg and 2.42 × 10<sup>3</sup> mm<sup>2</sup> kg mm<sup>-3</sup> (50). Lu *et al.* conducted research on the slurry erosion characteristics of three materials, including NiCoCrFeNb<sub>0.45</sub> eutectic HEA, mild carbon steel 1045 and stainless steel. The experiments were performed using a rotary jet erosion test machine and the results showed that erosion increased with higher velocities. The reason behind this is that the higher impact velocity increases the kinetic energy of sand particles, leading to a greater number of sand particles hitting the sample surface within a given time frame. On the other hand, a decrease in impact angle reduces erosion, suggesting that ablation is mainly influenced by head-on shock and cutting forces. Eutectic HEA showed better erosion resistance under all test conditions (51). In their study, Nair *et al.* investigated the cavitation

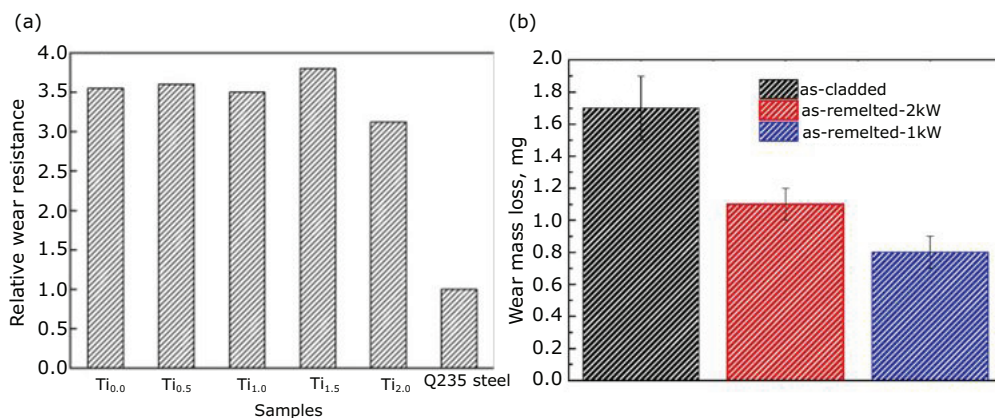


Fig. 4. (a) Comparison of relative wear resistance of Q235 steel and Al<sub>2</sub>CrFeCoCuNiTi<sub>x</sub> HEA coatings. Reprinted from (43) with permission from Elsevier; (b) wear mass loss comparison of as-cladded and as-remelted at 2 kW and 1 kW Ni-Cr-Co-Ti-V HEA (48)

erosion behaviour of  $\text{Al}_{0.1}\text{CrCoFeNi}$  high-entropy alloy and 316L stainless steel in a deionised water environment containing 3.5% sodium chloride. The experiments were conducted using a vibrating tip with a frequency of  $20 \pm 0.5$  kHz. The results demonstrated that the first signs of erosion were observed in 316L stainless steel after 2.7 h of exposure to distilled water. In contrast, the HEA coatings exhibited erosion after a significantly longer duration of 6.21 h. The HEA exhibited a volumetric erosive rate that was 10 times lower compared to the untreated 316L stainless steel substrate (52).

In summary, the evaluation of HEAs involves the study of various properties, such as microstructure, mechanical, thermal, electrical, wear, corrosion and magnetic properties, to understand their potential applications. Techniques like scanning electron microscopy and XRD are used to analyse the grain size, phase composition and elemental distribution. Mechanical properties, such as tensile strength, compressive strength and hardness, are studied using techniques like tensile testing and nanoindentation. Differential scanning calorimetry and thermal conductivity measurements are commonly employed techniques to assess thermal properties, including thermal conductivity and coefficient of thermal expansion. Electrical conductivity and resistivity can be measured using four-point probe techniques. Wear behaviour can be evaluated using tribological tests and corrosion resistance can be studied using electrochemical techniques. Magnetic properties can be analysed using techniques like vibrating sample magnetometry and magnetic force microscopy. Overall, the evaluation of HEAs properties is crucial in determining their potential applications in various industries such as aerospace, automotive and electronics. Understanding these properties can help researchers and manufacturers optimise HEA compositions for specific applications, leading to improved performance and efficiency of materials.

## 2. Applications of High Entropy Alloys

### 2.1 High Temperature Applications

The materials used in the aerospace industry, particularly those used to make engine parts, are subjected to extreme operating conditions at very high temperatures. As a result, the materials used should be light in weight and have very good strength at elevated temperatures, as well as resistance to fatigue failure, wear, high-temperature oxidation

and chemical degradation. Current advancements in HEAs are focused primarily on their use in high-temperature applications. At these high temperatures, HEAs must not only withstand the harsh conditions but also behave admirably. In today's high-temperature environments, a large number of components are used. As a result, it is critical to investigate the behaviour of materials used in the manufacture of these components used in high-temperature applications. For instance, the performance of a jet engine will be improved when it is operated at an elevated temperature (53, 54). Furthermore, at high temperatures, the amount of fuel consumed in the oil and gas industries is significantly reduced. Aside from that, there are numerous high-temperature applications. As a result, materials that can operate at high temperatures are in high demand. Within the temperature range of 773 K to 873 K, the dual-phase  $\text{AlCoCrFeNi}$  alloy exhibits exceptional specific strength. Due to its lightweight properties, it has great potential in the field of structural applications of aerospace engines (55). The equimolar  $\text{VNbMoTa}$  RHEA has shown exceptional strength at high temperatures as well as good ductility at room temperature. This RHEA is also resistant to softening at high temperatures of up to 1000°C.

These characteristics make  $\text{VNbMoTa}$  RHEA a highly promising material for high-temperature applications (56). When compared to  $\text{HfNbTaTiZr}$ ,  $\text{HfNbTaTiZrW}$  and  $\text{HfNbTaTiZrMoW}$  RHEAs demonstrate higher yield strengths and more balanced mechanical properties at elevated

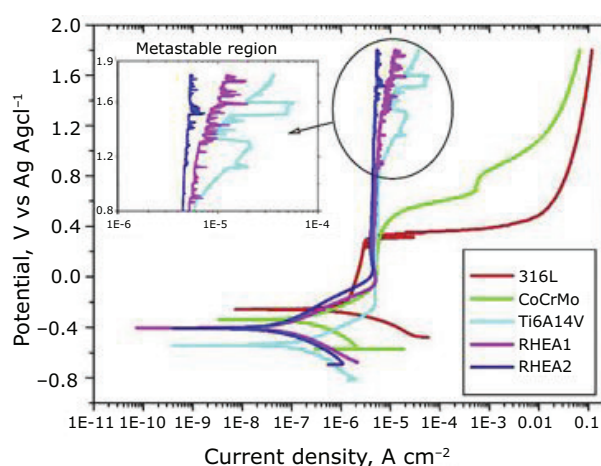


Fig. 5. Potentiodynamic curve of 316L, CoCrMo,  $\text{Ti}_6\text{Al}_4\text{V}$ , RHEA1 and RHEA2 in the PBS electrolyte at 37°C with a scan rate of  $1 \text{ mV s}^{-1}$ . Reprinted from (62) with permission from Elsevier

temperatures. The substantial improvements in strength observed in HfNbTaTiZrW and HfNbTaTiZrMoW RHEAs are attributed to their dual bcc structures, as well as the potent solid solution strengthening effect that results from the addition of tungsten or molybdenum. The restricted ductility of these RHEAs limits their industrial applications (57). In this regard, Xu *et al.* (58) prepared low-density  $Ti_{50-x}Al_xVNbMo$  RHEAs using an arc melting process. These alloys had very good strength and plasticity at high temperatures, as well as a low density. As a result, these RHEAs stand out as a strong contender for use in high-temperature applications, with potential advantages including increased energy efficiency, improved mechanical properties and good machinability.

## 2.2 Biomedical Applications

Desirable properties for a material to be considered biocompatible are high ductility, fatigue resistance and yield strength and it should also have a low modulus of elasticity. Tribological properties also influence whether a particular material is suitable for bio-implants. The most commonly used alloy as a biomaterial is  $Ti_6Al_4V$  (59). As a result, while developing new bio-compatible materials for comparison, this alloy is considered a standard material. As a result of the addition of niobium, tantalum and zirconium elements, the overall corrosion resistance of TiZrNbTaFe alloys prepared using powder metallurgy is much higher than that of  $Ti_6Al_4V$  (60). Thus, this new HEA can be considered a viable option for producing biomedical devices. Impact loading on BCC structured TiTaHfNb, TiTaHfNbZr and TiTaHfMoZr HEAs reveals that these alloys have lower Young's modulus than that of conventional materials that are used for implants. TiTaHfNb alloys may be a viable alternative for implant materials requiring high wear and corrosion resistance (61). Studies carried out in TiZrTaHfNb and  $Ti_{1.5}ZrTa_{0.5}Hf_{0.5}Nb_{0.5}$  RHEAs synthesised using arc melting process reveal properties like wear resistance, pitting and corrosion resistance and wettability are much better than that of conventional biomaterial like  $Ti_6Al_4V$  and thus can be used as a suitable substitute biomaterial (62).

Experimental studies (in **Table VI**) on as-cast TiZrNbTaMo HEA show that when compared to conventional orthopaedic alloys, its corrosion resistance is almost identical to that of  $Ti_6Al_4V$  and pitting resistance is better than that of 316L stainless steel and CoCrMo alloys (63). As a result, the proposed HEA can be investigated further for use as an alternative to conventional alloys. Titanium is the most common base material in biomedical HEAs. However, desired properties can be obtained by modifying the synthesis process and constituent components.

## 2.3 Nuclear Applications

Due to their high cost, HEAs face significant challenges in competing with common alloys such as aluminium alloys and steel in everyday structural applications. However, HEAs are suitable candidates for situations where high demands and challenging environmental conditions make conventional materials ineffective. One such field where HEAs have high potential is in the area of nuclear power generation. The requirements for materials used in nuclear reactors include low activation with minimal impurities, which enables the safe decommissioning and recycling of materials after the useful life of the reactor. For fusion reactors, this is an essential design criterion. HEAs, with their unique properties, have the potential to meet these requirements and provide a viable alternative to conventional materials. In addition to nuclear power generation, HEAs have shown promise in other demanding applications, such as aerospace, defence and high-temperature and corrosive environments. The unparalleled properties of HEAs make them particularly appealing for applications where conventional materials fail to meet the required criteria (64, 65).

TiVZrTa and TiVCrTa alloys consist of low-activation elements. These alloys have properties that are comparable with that of TiVNbTa alloy, as inferred from **Figures 6** and **7**. These alloys display enhanced radiation resistance regarding irradiation-induced hardening (66). Therefore, while HEAs may find it challenging to compete with common alloys in everyday applications,

**Table VI Electrochemical Properties of TiZrNbTaMo HEA Measured in PBS Solution with Conventional Biomedical Materials (63)**

| Alloy                                  | TiZrNbTaMo   | Ti <sub>6</sub> Al <sub>4</sub> V | 316 LSS      | CoCrMo       |
|--|--------------|-----------------------------------|--------------|--------------|
| E <sub>corr</sub> (mV <sub>sce</sub> ) | -607 (±55)   | -571 (±11)                        | -234 (±13)   | -320 (±30)   |
| I <sub>p</sub> (µA/cm <sup>2</sup> )   | 0.89 (±0.06) | 0.96 (±0.21)                      | 0.83 (±0.03) | 0.42 (±0.19) |

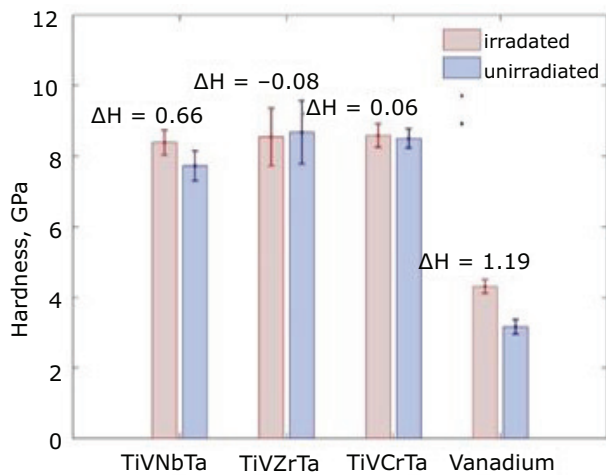


Fig. 6. Indentation hardness of irradiated and unirradiated HEAs and control sample at 300 nm indentation depth. Reprinted from (66) under Creative Commons attribution License 4.0 (CC-BY 4.0)

they present a promising alternative in situations where conventional materials fail to meet the requirements. With further research and development, HEAs have the potential to become a viable alternative to conventional materials in a wide range of demanding applications.

### 2.4 Automotive applications

HEAs exhibit a distinctive blend of mechanical, thermal and chemical properties, making them highly desirable for a range of automotive applications. These alloys can be effectively utilised in engine components, including pistons, cylinder liners and valves, due to their

remarkable high-temperature stability, wear resistance and low thermal expansion coefficient. The exceptional high-temperature stability of HEAs provides significant advantages for engine components that experience elevated temperatures during operation. Moreover, HEAs find potential applications in exhaust systems, where materials with high corrosion resistance and good thermal stability are required. The excellent corrosion resistance of HEAs makes them an ideal choice for use in harsh environments typically encountered in exhaust systems. Furthermore, HEAs offer opportunities in lightweighting applications, where their high strength-to-weight ratio proves advantageous for reducing vehicle weight and enhancing fuel efficiency. These alloys contribute to achieving weight reduction objectives while maintaining the necessary structural integrity.

Additionally, HEAs can be used in safety-related applications, such as crash-resistant structures, where their high ductility and energy absorption capacity can provide improved safety performance. HEAs have the potential to enable the development of lightweight and energy-efficient vehicles without compromising on safety. Overall, the distinctive and advantageous properties of HEAs position them as promising contenders for a wide range of automotive applications. Further research is needed to optimise their properties for specific applications and to develop cost-effective manufacturing processes for HEA components. With continued research and development, the potential impact of HEAs on the automotive industry is indeed significant, with the possibility of revolutionising vehicle development in terms of safety, efficiency and environmental friendliness.

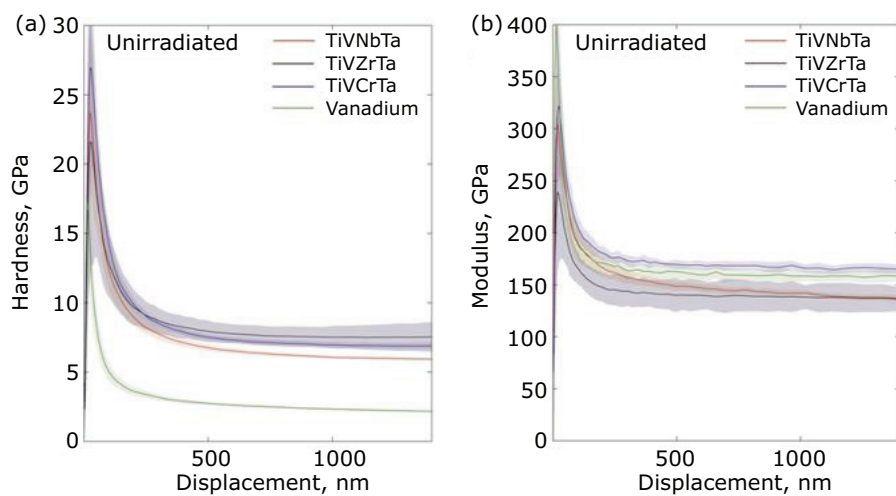


Fig. 7. (a) Unirradiated indentation hardness vs. depth; (b) unirradiated indentation modulus vs. depth. Reprinted from (66) under Creative Commons attribution License 4.0 (CC-BY 4.0)

## 2.5 Energy Storage Applications

Hydrogen is an alternative, renewable energy source that has the potential to reduce our reliance on fossil fuels for meeting our energy requirements. Metal hydrides have been explored as a means of solid hydrogen storage, primarily due to their high-volume storage capacity and safety features. However, magnesium-based metal hydrides require elevated temperatures for efficient hydrogen absorption and release, primarily due to their unfavourable kinetics during the hydrogen absorption and desorption processes (67, 68). HEAs are emerging as suitable substitutes for hydrogen storage owing to their ability to form multicomponent solid solutions and other (69, 8, 68, 70). Research has shown that bcc phase MgAlTiFeNi HEA synthesised using high energy ball milling processes exhibits a practical storage capacity of 0.94 wt% for storing hydrogen and exhibits excellent hydrogen absorption and desorption kinetics (71). This HEA has tremendous potential as a hydrogen storage material and further research in this area is ongoing. The use of HEAs for hydrogen storage offers several advantages over traditional metal hydrides, such as improved kinetics and lower operating temperatures. These properties make HEAs a promising alternative for hydrogen storage, which could significantly increase the use of hydrogen as a renewable energy source. With further research and development, HEAs could play a crucial role in the transition towards a more sustainable energy future.

To summarise, the notable high-temperature characteristics of HEAs, including their elevated melting points and exceptional thermal stability, make them appealing for implementation in various high-temperature settings such as gas turbines, rocket nozzles and other environments with extreme heat. Furthermore, HEAs exhibit promising potential for biomedical applications owing to their exceptional biocompatibility and resistance to corrosion. In nuclear applications, the high density and favourable mechanical properties of HEAs make them suitable for applications in radiation shielding. In the automotive industry, HEAs can be used to reduce weight while maintaining strength and durability. Finally, HEAs have shown potential for energy storage applications, such as in battery electrodes, due to their high electrical conductivity and capacity for reversible lithium-ion storage.

## 3. Challenges and Future Directions

Multiple principal elements are mixed together in the crystal lattice to form HEAs. These alloys are commonly referred to as solid solution alloys, but the distinction between solvents and solutes is unclear. Consequently, understanding HEAs becomes challenging using existing theories on solid solution strengthening mechanisms. Due to the inclusion of multiple primary elements with diverse atomic sizes and chemical properties, HEAs exhibit a highly distorted crystallographic lattice structure. This distinctive feature sets them apart from conventional alloys and introduces unique behaviours in terms of crystal defects. To establish the relationship between microstructure and mechanical properties in HEAs, it is necessary to employ new characterisation techniques, advanced computation methods and conduct extensive experimental work. These novel approaches will enable researchers to understand and analyse the complex structure of these alloys, as well as their corresponding mechanical behaviour. Additionally, achieving HEAs with improved properties presents a critical challenge in the field of materials science. Overcoming the hurdle of obtaining a uniform composition, microstructure and properties in HEAs during the fabrication process is of utmost importance. This challenge arises due to the presence of numerous constituent elements in HEAs, each with diverse atomic sizes and chemical properties. Consequently, achieving a homogenised distribution of these elements within the alloy becomes difficult. To ensure consistency in microstructure and properties throughout the material, meticulous control of the fabrication process is necessary. However, the current synthesis methods for HEAs are limited and require improvement to achieve a more uniform composition, microstructure and properties. Novel synthesis methods will be required to address this goal effectively. Various advanced processing techniques, such as spark plasma sintering, severe plastic deformation and rapid solidification, have been proposed to optimise the properties and microstructure of HEAs. However, to develop effective methods for optimising HEAs, a deeper understanding of the underlying mechanisms governing their formation and stability is needed. In the future, HEA research will focus on developing advanced processing techniques to optimise microstructures and properties. Achieving a comprehensive understanding of the fundamental mechanisms involved in the formation and stability of HEAs will require a combination of experimental and theoretical approaches. Ultimately, this knowledge

will enable the design of new HEAs with improved properties for a wide range of applications.

Besides, HEAs possess immense potential for various applications in sectors such as aerospace, energy and biomedical fields, among others. In the aerospace industry, their exceptional mechanical properties, high-temperature stability and corrosion resistance make them highly suitable for turbine blades, heat exchangers and other critical components. HEAs are actively being explored for energy applications, specifically in high-temperature environments like nuclear reactors, thermal power plants and other situations that demand materials with superior performance at elevated temperatures. In the biomedical field, HEAs are under investigation for their potential use in implantable medical devices, primarily due to their biocompatibility and mechanical properties. The unique combination of properties offered by HEAs positions them as promising candidates for a wide range of advanced applications. However, further research is essential to fully explore their potential in existing applications and to develop new ones. By investing in continued research, we can unlock the full potential of HEAs and expedite the development of advanced materials that offer superior performance and enhanced functionality.

As with any new material, addressing the sustainability of HEAs is crucial. This entails examining their environmental impact and developing more sustainable production methods. The production of HEAs typically involves high temperatures and energy-intensive processes, which can lead to substantial greenhouse gas emissions and other environmental consequences. Thus, it is important to explore alternative production methods that minimise the environmental impact associated with HEAs. Furthermore, it is essential to thoroughly investigate the long-term environmental impact of HEAs, including their potential toxicity and effects on ecosystems. By conducting comprehensive studies on these aspects, we can better understand and mitigate any potential negative consequences. Through the pursuit of sustainable practices in the development and use of HEAs, we can ensure that these materials are produced and utilised in a responsible and environmentally conscious manner.

Based on the information provided by other studies, future recommendations for HEAs will focus on several key areas. Firstly, there is a need to unify and standardise the terminology used to describe HEAs, as well as the test methods and reported data structures. This standardisation

will facilitate easier comparison of results and data processing. Secondly, the development of a global relational database is recommended. This database should contain digitised detailed information on the composition, manufacturing methods, testing and results of HEAs. Such a database would enable statistical data processing and the tracing of composition-processing-structure-properties interdependencies. Thirdly, it is crucial to develop procedures for processing and surface engineering of HEAs. This will enable the fabrication of complex-shaped products, including the use of AM methods. Additionally, the economic and environmental viability of HEAs should be addressed to assess their feasibility for various applications. This consideration will help determine the practicality and sustainability of implementing HEAs in different industries. Furthermore, research should be conducted to investigate the thermophysical properties of HEAs, such as elastic constants, diffusion coefficients, heat capacity and thermal conductivity. Understanding these properties will provide valuable insights into the behaviour of HEAs in different applications. Lastly, exploring new potential applications for HEAs, beyond their current proposed uses, such as in electronic devices or catalysis, is recommended. Investigating these unexplored areas will contribute to expanding the horizons of HEA applications. Addressing these future points will facilitate the advancement of understanding and development of HEAs, paving the way for their successful implementation in various industries.

#### 4. Summary and Conclusion

In summary, the field of HEAs is a rapidly emerging one, with an ever-increasing number of new alloy systems being developed. There is only a little progress made in understanding the alloy system fully. A deeper understanding of the potential of HEAs requires further exploration of additional elements and combinations. Irrespective of the complex processing methods required for developing HEAs and the high entropy of mixing, the resulting phase structure is often a simple solid solution. With various new processing methods adopted in developing HEAs, it will be interesting to know how these methods influence the solid solutions developed. The research data available on the mechanical properties of HEAs predominantly focus on hardness and compressive strengths. The surface hardness of the substrate material can be improved significantly by providing the HEA coatings to it. There is only a limited work carried out in the area of tensile properties of HEAs.

Hence more work has to be carried out in this area to clearly understand how HEAs behave when it is subjected to tensile loading. Magnetic properties of HEAs can be manipulated according to the required application by adding various alloying elements like aluminium, copper, chromium and others to the FeCoNi alloy system. Various HEAs demonstrated excellent corrosion resistance when exposed to highly corrosive environments. Because of these unique properties, HEAs are a suitable alternative material in high-temperature, nuclear, energy storage and corrosive environment applications.

Through a comprehensive review of microstructure, properties and applications, it becomes evident that HEAs possess unique characteristics that distinguish them from conventional alloys. Their remarkable stability, mechanical strength and resistance to wear and corrosion make them highly promising candidates for a wide range of applications. The microstructural diversity exhibited by HEAs, arising from their multicomponent nature, presents an intriguing avenue for tailoring material properties to specific needs. The synergistic effects of various alloying elements contribute to the formation of complex structures, which in turn influence mechanical, thermal and magnetic properties. Understanding and controlling these microstructures are crucial for harnessing the full potential of HEAs in practical applications. Ongoing research endeavours continue to refine our knowledge of these alloys, offering the potential for breakthroughs in performance and efficiency. However, despite the significant strides made in the field of HEAs, there are still challenges and unanswered questions that warrant further investigation.

Areas that merit continued research include the scalability of production methods, ensuring long-term stability of HEAs and optimising alloy compositions for specific applications. By delving deeper into these aspects, valuable insights can be gained, leading to advancements in the field. In summary, the exploration of HEAs unveils their capacity to revolutionise materials engineering. The interplay between microstructure, properties and applications weaves a rich tapestry of possibilities. As our understanding deepens, so does the potential for HEAs to redefine the boundaries of what is achievable in modern materials science.

## References

1. S. Arun, N. Radhika, B. Saleh, *Johnson Matthey Technol. Rev.*, 2024, **68**, (4), 549
2. M. E. McHenry, M. A. Willard, D. E. Laughlin, *Prog. Mater. Sci.*, 1999, **44**, (4), 291
3. M. E. McHenry, D. E. Laughlin, *Acta Mater.*, 2000, **48**, (1), 223
4. O. Gutfleisch, M. A. Willard, E. Brück, C. H. Chen, S. G. Sankar, J. P. Liu, *Adv. Mater.*, 2011, **23**, (7), 821
5. P. Kumari, A. K. Gupta, R. K. Mishra, M. S. Ahmad, R. R. Shahi, *J. Magn. Magn. Mater.*, 2022, **554**, 169142
6. V. Chaudhary, R. Chaudhary, R. Banerjee, R. V Ramanujan, *Mater. Today*, 2021, **49**, 231
7. M.-H. Tsai, *Entropy*, 2013, **15**, (12), 5338
8. D. B. Miracle, O. N. Senkov, *Acta Mater.*, 2017, **122**, 448
9. T. T. Zuo, R. B. Li, X. J. Ren, Y. Zhang, *J. Magn. Magn. Mater.*, 2014, **371**, 60
10. F. Alijani, M. Reihanian, Kh. Gheisari, *J. Alloys Compd.*, 2019, **773**, 623
11. R.-F. Zhao, B. Ren, G.-P. Zhang, Z.-X. Liu, J. Zhang, *J. Magn. Magn. Mater.*, 2018, **468**, 14
12. T. Zuo, M. C. Gao, L. Ouyang, X. Yang, Y. Cheng, R. Feng, S. Chen, P. K. Liaw, J. A. Hawk, Y. Zhang, *Acta Mater.*, 2017, **130**, 10
13. Z. Li, G. Bai, X. Liu, S. Bandaru, Z. Wu, X. Zhang, M. Yan, H. Xu, *J. Alloys Compd.*, 2020, **845**, 156204
14. R. K. Mishra, R. R. Shahi, *J. Magn. Magn. Mater.*, 2017, **442**, 218
15. S. Singh, N. Wanderka, K. Kiefer, K. Siemensemeyer, J. Banhart, *Ultramicroscopy*, 2011, **111**, (6), 619
16. K. Huang, G. Wang, H. Qing, Y. Chen, H. Guo, *Vacuum*, 2022, **195**, 110695
17. G. Zhang, Q. Zhan, K. Zheng, J. Tang, B. Cai, Z. Liu, *Ceram. Int.*, 2023, **49**, (1), 808
18. Y.-Y. Chen, S.-B. Hung, C.-J. Wang, W.-C. Wei, J.-W. Lee, *Surf. Coatings Technol.*, 2019, **375**, 854
19. A. Xia, R. Franz, *Coatings*, 2020, **10**, (10), 941
20. M. S. Jadhav, D. Sahane, A. Verma, S. Singh, *Adv. Powder Technol.*, 2021, **32**, (2), 378
21. S. A. Uporov, R. E. Ryltsev, V. A. Sidorov, S. Kh. Estemirova, E. V. Sterkhov, I. A. Balyakin, N. M. Chhtchelkatchev, *Intermetallics*, 2022, **140**, 107394
22. H. Tanimoto, R. Hozumi, M. Kawamura, *J. Alloys Compd.*, 2022, **896**, 163059
23. H. Kim, S. Nam, A. Roh, M. Son, M.-H. Ham, J.-H. Kim, H. Choi, *Int. J. Refract. Met. Hard Mater.*, 2019, **80**, 286
24. Y. Zhang, G. M. Stocks, K. Jin, C. Lu, H. Bei, B. C. Sales, L. Wang, L. K. Béland, R. E. Stoller, G. D. Samolyuk, M. Caro, A. Caro, W. J. Weber, *Nat. Commun.*, 2015, **6**, 8736
25. X. Feng, J. Zhang, Z. Xia, W. Fu, K. Wu, G. Liu, J. Sun, *Mater Lett.*, 2018, **210**, 84
26. Z. Rong, C. Wang, Y. Wang, M. Dong, Y. You, J. Wang, H. Liu, J. Liu, Y. Wang, Z. Zhu, *J. Alloys Compd.*, 2022, **921**, 166061

27. Y.-J. Hsu, W.-C. Chiang, J.-K. Wu, *Mater. Chem. Phys.*, 2005, **92**, (1), 112
28. M. Tan, L. Meng, C. Lin, L. Ke, Y. Liu, J. Qu, T. Qi, *J. Alloys Compd.*, 2022, **927**, 167081
29. W. Wang, W. Qi, L. Xie, X. Yang, J. Li, Y. Zhang, *Materials*, 2019, **12**, (5), 694
30. Y. Shi, B. Yang, X. Xie, J. Brechtel, K. A. Dahmen, P. K. Liaw, *Corros. Sci.*, 2017, **119**, 33
31. Z. Zhou, L. Wang, X. Zhao, J. Wu, F. Zhang, J. Pi, *Surf. Interfaces*, 2021, **23**, 100956
32. A. Raza, S. Abdulahad, B. Kang, H. J. Ryu, S. H. Hong, *Appl. Surf. Sci.*, 2019, **485**, 368
33. Y. Shi, L. Collins, R. Feng, C. Zhang, N. Balke, P. K. Liaw, B. Yang, *Corros. Sci.*, 2018, **133**, 120
34. S. Zhang, C. L. Wu, C. H. Zhang, M. Guan, J. Z. Tan, *Opt. Laser Technol.*, 2016, **84**, 23
35. Y. Li, Y. Shi, *Opt. Laser Technol.*, 2021, **134**, 106632
36. P. Muangtong, A. Rodchanarowan, D. Chaysuwan, N. Chanlek, R. Goodall, *Corros. Sci.*, 2020, **172**, 108740
37. W. Muftah, J. Allport, V. Vishnyakov, *Surf. Coatings Technol.*, 2021, **422**, 127486
38. D. H. Xiao, P. F. Zhou, W. Q. Wu, H. Y. Diao, M. C. Gao, M. Song, P. K. Liaw, *Mater. Des.*, 2017, **116**, 438
39. Y. L. Chou, J. W. Yeh, H. C. Shih, *Corros. Sci.*, 2010, **52**, (8), 2571
40. Y. Yao, Y. Jin, W. Gao, X. Liang, J. Chen, S. Zhu, *Metals*, 2021, **11**, (9), 1471
41. P. Wu, K. Gan, D. Yan, Z. Fu, Z. Li, *Corros. Sci.*, 2021, **183**, 109341
42. X. Ye, M. Ma, Y. Cao, W. Liu, X. Ye, Y. Gu, *Phys. Procedia*, 2011, **12**, (A), 303
43. X. W. Qiu, Y. P. Zhang, C. G. Liu, *J. Alloys Compd.*, 2014, **585**, 282
44. H. A. Aly, K. A. Abdelghafar, G. A. Gaber, L. Z. Mohamed, *J. Mater. Eng. Perform.*, 2021, **30**, (2), 1430
45. Y. Wang, Y. Yang, H. Yang, M. Zhang, S. Ma, J. Qiao, *Mater. Chem. Phys.*, 2018, **210**, 233
46. J.-K. Xiao, Y.-Q. Wu, J. Chen, C. Zhang, *Wear*, 2020, **448–449**, 203209
47. B. Jin, N. Zhang, H. Yu, D. Hao, Y. Ma, *Surf. Coatings Technol.*, 2020, **402**, 126328
48. Z. Cai, X. Cui, Z. Liu, Y. Li, M. Dong, G. Jin, *Opt. Laser Technol.*, 2018, **99**, 276
49. C. Huang, Y. Zhang, R. Vilar, J. Shen, *Mater. Des.*, 2012, **41**, 338
50. X. Ji, C. Ji, J. Cheng, Y. Shan, S. Tian, *Wear*, 2018, **398–399**, 178
51. J. Lu, Z. Wang, W. Wang, K. Zhou, F. He, Z. Wang, *Acta Metall. Sin. (Eng. Lett.)*, 2020, **33**, (8), 1111
52. R. B. Nair, H. S. Arora, S. Mukherjee, S. Singh, H. Singh, H. S. Grewal, *Ultrason. Sonochem.*, 2018, **41**, 252
53. J. Chen, X. Zhou, W. Wang, B. Liu, Y. Lv, W. Yang, D. Xu, Y. Liu, *J. Alloys Compd.*, 2018, **760**, 15
54. S. K. Dewangan, A. Mangish, S. Kumar, A. Sharma, B. Ahn, V. Kumar, *Eng. Sci. Technol. Int. J.*, 2022, **35**, 101211
55. K. R. Lim, K. S. Lee, J. S. Lee, J. Y. Kim, H. J. Chang, Y. S. Na, *J. Alloys Compd.*, 2017, **728**, 1235
56. M. Wang, Z. L. Ma, Z. Q. Xu, X. W. Cheng, *Scr. Mater.*, 2021, **191**, 131
57. M. Wang, Z. Ma, Z. Xu, X. Cheng, *J. Alloys Compd.*, 2019, **803**, 778
58. Z. Q. Xu, Z. L. Ma, M. Wang, Y. W. Chen, Y. D. Tan, X. W. Cheng, *Mater. Sci. Eng.: A*, 2019, **755**, 318
59. J. P. Oliveira, B. Panton, Z. Zeng, C. M. Andrei, Y. Zhou, R. M. Miranda, F. M. B. Fernandes, *Acta Mater.*, 2016, **105**, 9
60. G. Popescu, B. Ghiban, C. A. Popescu, L. Rosu, R. Truscă, I. Carcea, V. Soare, D. Dumitrescu, I. Constantin, M. T. Olaru, B. A. Carlan, *IOP Conf. Ser.: Mater. Sci. Eng.*, 2018, **400**, 022049
61. S. Gurel, M. B. Yagci, D. Canadinc, G. Gerstein, B. Bal, H. J. Maier, *Mater. Sci. Eng.: A*, 2021, **803**, 140456
62. A. Motallebzadeh, N. S. Peighambaroust, S. Sheikh, H. Murakami, S. Guo, D. Canadinc, *Intermetallics*, 2019, **113**, 106572
63. S.-P. Wang, J. Xu, *Mater. Sci. Eng.: C*, 2017, **73**, 80
64. Y. Seki, T. Tabara, I. Aoki, S. Ueda, S. Nishio, R. Kurihara, *J. Nucl. Mater.*, 1998, **258–263**, (2), 1791
65. E. J. Pickering, A. W. Carruthers, P. J. Barron, S. C. Middleburgh, D. E. J. Armstrong, A. S. Gandy, *Entropy*, 2021, **23**, (1), 98
66. A. Kareer, J. C. Waite, B. Li, A. Couet, D. E. J. Armstrong, A. J. Wilkinson, *J. Nucl. Mater.*, 2019, **526**, 151744
67. B. Sakintuna, F. Lamari-Darkrim, M. Hirscher, *Int. J. Hydrogen Energy*, 2007, **32**, (9), 1121
68. A. Züttel, *Mater. Today*, 2003, **6**, (9), 24
69. J.-W. Yeh, *Ann. Chim. Sci. Mater.*, 2006, **31**, (6), 633
70. Y. Zhang, T. T. Zuo, Z. Tang, M. C. Gao, K. A. Dahmen, P. K. Liaw, Z. P. Lu, *Prog. Mater. Sci.*, 2014, **61**, 1
71. K. R. Cardoso, V. Roche, A. M. Jorge, F. J. Antiquera, G. Zepon, Y. Champion, *J. Alloys Compd.*, 2021, **858**, 158357

### Conflicts of Interest

The authors reported no potential conflict of interest.

## The Authors



S. Arun is a PhD Research Scholar, under the guidance of N. Radhika, Department of Mechanical Engineering, Amrita School of Engineering, Amrita Vishwa Vidyapeetham, Coimbatore, India. His current research focuses of microstructure, properties and application of HEA fabricated using vacuum arc melting process.



N. Radhika currently serves as Professor at the Department of Mechanical Engineering, Amrita School of Engineering, Coimbatore, India. Her areas of research include composite materials, metal matrix composites, HEAs, functionally graded materials, optimisation techniques, heat treatment process and tribological characteristics. She has published more than 150 research papers in reputed international journals.



Bassiouny Saleh obtained his PhD in engineering mechanics at the College of Mechanics and Materials, Hohai University (HHU), Nanjing, China, in 2021. With a research background in material science and technology spanning over ten years, he has amassed extensive expertise in the field. From January 2022 to May 2023, Saleh worked as a postdoctoral researcher at HHU. Currently, he holds the position of postdoctoral researcher in the College of Energy and Power Engineering at Nanjing University of Aeronautics and Astronautics since June 2023. His current research interests revolve around functionally graded materials, metal matrix composites, AM, severe plastic deformation, HEAs, wear, casting and corrosion analysis. Saleh has contributed significantly to the scientific community, co-authoring 60 publications indexed in the Web of Science. His research work has garnered an h-index of 18 and an i10-index of 25, with over 1450 citations as of December 2023.